RSC Advances

ROYAL SOCIETY OF CHEMISTRY

www.rsc.org/advances

Magnetic dynamics of two salen type Dy$_2$ complexes modulated by coordination geometry

Xiaoyan Zou, Pengfei Yan*, Yanping Dong, Fang Luan, Guangming Li*

Key Laboratory of Functional Inorganic Material Chemistry (MOE); School of Chemistry and Materials Science, Heilongjiang University, Harbin 150080, P. R. China. Fax: 86-451-86673647; Tel.: 86-451-86608458; E-mail: gmli_2000@163.com.

Abstract

Two salen type dinuclear dysprosium complexes, namely, [Dy(H$_2$L)(NO$_3$)$_3$]$_2$·CH$_2$Cl$_2$·CH$_3$OH·H$_2$O (**1**) and [Dy(H$_2$L^1)$_2$(NO$_3$)$_3$]$_2$·2CH$_2$Cl$_2$·2CH$_3$OH (**2**); [H$_2$L = *N,N'*-(1,3-propylene)bis(3-methoxysalicylideneimine) and H$_2$L^1 = *N,N'*-(1,3-propylene)bis(salicylideneimine)], have been isolated by reactions of Dy(NO$_3$)$_3$·6H$_2$O with two different but similar salen types (H$_2$L and H$_2$L^1) , respectively. X-ray crystallographic analyses reveal that two crystallographically equivalent Dy(III) ions for **1** and two crystallographically non-equivalent Dy(III) ions for **2** were both bridged by two ligands displaying the broken hula hoop-like and hula hoop-like coordination geometry, which result in the distinct magnetic properties that complex **2** exhibited relatively higher energy barriers under 2 K Oe dc field for complexes **1** and **2,** respectively.

Introduction

Single molecule magnets of the homo-multinuclear lanthanide complexes continue to be attractive owing to their potential applications for the uses of high-density magnetic memories, molecular spintronics and quantum computing devices.[1] Particular attention has been devoted to Dy(III) ion, attributed to the inherently large magnetic moment with a Kramers ground state of ^{6}H$_{15/2}$ and a large Ising-type magnetic anisotropy. It has indisputably led to the largest

number of pure 4f SMMs with various nuclear.[2] Among the SMMs of Dy(III) complexes, the recorded effective energy barrier was 528 K reported by Blagg R. J. et al. in 2011.[3] It demonstrated that the ligands played essential roles to achieve SMMs by way of ligand field and defined geometries.[4] Among numerous ligands, salen type with rich oxygen and nitrogen donors have been widely used in the construction of polynuclear d-4f and 4f complexes [5] and can stabilize different Dy(III) ions in various coordination environments displaying distinct anisotropic centers, such as mononuclear,[6] dinuclear,[2e, 7] tetranuclear,[8] and 1D chain,[9] etc. Among the reported SMMs of salen-type Dy(III)-based complexes, the dinuclear Dy_2 complexes exhibited relatively higher energy barriers, e.g. Long and co-workers have reported a centrosymmetric salen type dinuclear complex $[Dy_2(valdien)_2](NO_3)_2]$ (H_2valdien = N_1,N_3-bis(-3-methoxysalicylidene)diethylenetriamine) with a anisotropy barrier of 76 K in 2011,[7d] a asymmetric salen type dinuclear complex $(NEt_4)_2[Dy_2(L^2)_4](H_2O)(DMF)_{0.5}$ (H_2L^2 = N,N'-bis(-3-methoxybenzylidene)biphenyl-4,4′-diamine) that afford the recorded higher energy barrier of 101 K by controlling the magnetic axes in 2012,[7b] and a centrosymmetric salen type dinuclear complex $[Dy_2(valdien)_2](CF_3COCHCOCF_3)_2]$ (H_2valdien = N_1,N_3-bis(-3-methoxysalicylidene)diethylenetriamine) with a anisotropy barrier of 110 K by adding electron-withdrawing substitutes on the terminal ligands in a systematic fashion in 2013.[7a] Although considerable efforts have been dedicated to understand the correlationship of the magnetism-structure in these salen type Dy(III)-based SMMs,[4b] there are still great challenge to tell the origin of the slow magnetic relaxation of salen-type dinuclear Dy_2 complexes. In view of the recent important progress on the structure and magnetic of salen type lanthanide complexes[10] as well as our long-standing research on this domain,[11] attempting to explore the correlationship of magnetism-structure of salen type dinuclear Dy_2 complexes, two similar but different salen type ligand (H_2L and H_2L^1, Scheme 1) were thus employed in the experiment. As a result, two similar salen type Dy_2 complexes **1** and **2** have been isolated. Their correlationship of magnetism-structure have been described and discussed.

Experimental

Materials and physical measurements

H_2L and H_2L^1 were prepared according to the literature method.[12] $Dy(NO_3)_3 \cdot 6H_2O$ was prepared by the reactions of Dy_2O_3 and nitric acid in aqueous solution. Other chemicals were commercially available and used without further purification. Elemental (C, H and N) analyses were performed on a Perkin-Elmer 2400 analyzer. FT-IR data were collected on a Perkin-Elmer 100 spectrophotometer by using KBr pellet in the range of $4000{-}400$ cm^{-1}. UV spectra (in methanol) were recorded on a Perkin-Elmer Lambda 35 spectrophotometer. Thermal analyses were conducted on a Perkin-Elmer STA 6000 with a heating rate of 10 ºC· min^{-1} in a temperature range from 30 ºC to 800 ºC under atmosphere. Powder X-ray diffraction (PXRD) data were recorded on a Rigaku D/Max-3B X-ray diffractometer with CuKα as the radiation source (λ = 0.15406 nm) in the angular range θ = 5$-$50º at room temperature. The magnetic susceptibilities of complexes **1** and **2** were measured with a Quantum Design VSM superconducting interference device (SQUID) magnetometer. The magnetic corrections were made by using Pascal's constants.

Synthesis of complexes 1 and 2

$[Dy(H_2L)(NO_3)_3]_2 \cdot CH_2Cl_2 \cdot CH_3OH \cdot H_2O$ (**1**). A solution of $Dy(NO_3)_3 \cdot 6H_2O$ (0.094 g, 0.2 mmol) in MeOH (10 mL) was dropwise added to a solution of H_2L (0.068 g, 0.2 mmol) in CH_2Cl_2 (10 mL). The resulting solution was stored in the dark at ambient temperature. Yellow crystal was obtained in about one week. Yield: 0.106 g (70%). *Anal*. Calcd for $C_{40}H_{52}Cl_2N_{10}O_{28}Dy_2$ (1516.8): C, 31.67; H, 3.46; N, 9.23; Found: C, 32.62; H, 3.50; N, 9.19%. IR (KBr pellet, cm^{-1}): 3418 (w), 3104 (w), 1654 (vs), 1453 (s), 1285 (s), 1228 (s), 1099 (m), 1034 (m), 813 (m). UV-VIS [MeOH, λ_{max}]: 340, 265, 222 nm.

$[Dy(H_2L^1)_2(NO_3)_3]_2 \cdot 2CH_2Cl_2 \cdot 2CH_3OH$ (**2**). A solution of $Dy(NO_3)_3 \cdot 6H_2O$ (0.086 g, 0.20 mmol) in MeOH (10 mL) was dropwise added to a solution of H_2L^1 (0.118 g, 0.41 mmol) in CH_2Cl_2 (10 mL). The resulting solution was stored in the dark at ambient temperature. Yellow

crystal was obtained in about one week. Yield: 0.092 (45%). *Anal*. Calcd for

$C_{72}H_{84}Cl_4N_{14}O_{28}Dy_2$ (2060.33): C, 41.97; H, 4.11; N, 9.52%; Found: C, 41.90; H, 4.10; N,

9.50%. IR (KBr pellet, cm^{-1}): 3420 (w), 3055 (w), 1650 (vs), 1503 (s), 1287 (s), 1215 (s), 843

(m), 731 (m), 555 (m). UV-VIS [MeOH, λ_{max}]: 370, 262, 221 nm.

X−ray crystallography

Suitable single crystals of **1** and **2** were selected for X-ray diffraction analysis. Structural

analyses were performed on a Siemens SMART CCD diffractometer using

graphite-monochromated Mo-Kα radiation (λ = 0.71073 Å). Data processing was

accomplished with the SAINT processing program.[13] The structure was solved by direct

methods and all non-hydrogen atoms are anisotropically refined by full matrix least-squares

on F^2 using the SHELXTL-97 program.[14] The crystal data and structure refinements for

complexes **1** and **2** are listed in Table 1.
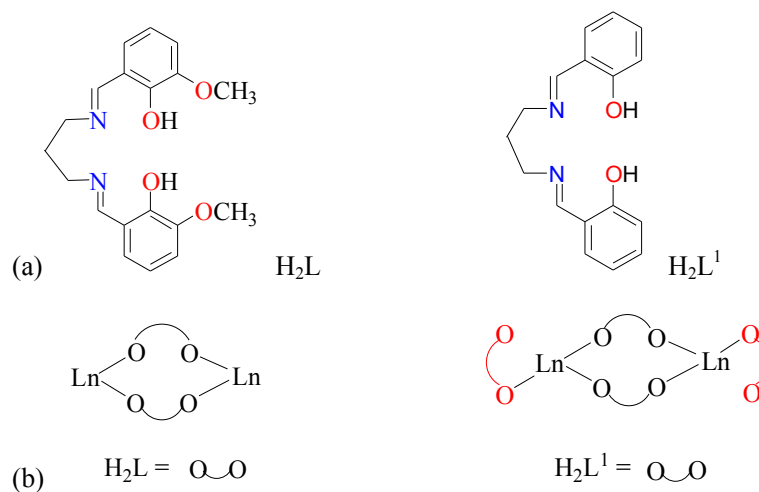
Scheme 1 (a) Schematic diagrams of ligands H_2L and H_2L^1; (b) Connection modes of two

ligands.

Table 1 Crystal data and structure refinements for complexes **1** and **2**

Complexes	**1**	**2**
Formula	$C_{40}H_{52}Cl_2N_{10}O_{28}Dy_2$	$C_{72}H_{84}Cl_4N_{14}O_{28}Dy_2$
Formula weight	1516.88	2060.33
Crystal system	Monoclinic	Triclinic
Space group	$P2_1/c$	$P\bar{1}$
a/Å	12.087(2)	10.963(2)
b/Å	14.937(3)	10.998(2)
c/Å	15.076(3)	18.653(4)
α (°)	90	92.00(3)
β (°)	98.45(3)	106.70(3)
γ (°)	90	92.49(3)
Z	2	1
V/Å^3	2692.3(9)	2149.4(7)
ρ/g cm^3	1.779	1.587
μ/mm^{-1}	2.852	1.934
F (000)	1428	1032
θ range /deg	3.00–27.47	3.01–25.00
Collected reflections	24527/6107	16938/12711
Unique $R_{(int)}$	0.0343	0.0312
R_a [I > 2σ(I)]	0.0371, 0.957	0.0403, 0.0966
R_a (all data)	0.0485, 0.1016	0.0513, 0.1023
GOF on F^2	1.066	1.068

Results and discussion

TG-DSC analysis

TG-DSC analysis of complexes **1** and **2** are showed in Figure S1, respectively. Complex **1** exhibits a gradual weight loss of 8.56% in the range of 30–217 ºC, which corresponds to the loss of one crystalline water molecule, one methanol and dichloromethane molecules (calcd 8.84%). Complex **2** exhibits a gradual weight loss of about 11.50%, which corresponds to the loss of two crystalline dichloromethane and methanol molecules (calcd 11.24%) in the range of 40–135 ºC. TG-DSC data further confirm that the crystalline solvents exist in complex **1** and **2**.

PXRD analysis

Powder X-ray diffraction (PXRD) patterns of complexes **1** and **2** are in agreement with the simulated ones (Figure S2). PXRD analysis further demonstrates that the crystal structures of complexes **1** and **2** are truly representative of the bulk materials. The differences in intensity are due to the preferred orientation of the powder samples.

Structural description of complexes 1 and 2

X-ray crystallographic analysis reveals that complex **1** crystallizes in a monoclinic space group of $P2_1/c$, possessing a neutral centrosymmetric structure (Figure 1, left). Complex **1** consists of two Dy(III) ions, six nitrate anion, two H_2L ligands. Two crystallographically equivalent Dy(III) ions are bridged by a pair of chelating oxygen atoms from phenoxo and methoxy groups of ligands (H_2L) with Dy1–Dy2 separation of 10.098 Å. Each Dy(III) ions are 10-coordinated by six oxygen atoms from three nitrate groups and four oxygen atoms from two H_2L ligands forming a distorted bi-capped square anti-prismatic geometry (Figure S3). The Dy–O bond lengths are in the range of 2.242(3)–2.804(3) Å. The bond lengths (2.242(3), 2.250(3) Å) from phenoxo are distinctively shorter than those from the methoxy groups (2.606(3) and 2.804(3) Å), respectively. The Dy–O distances of six oxygen atoms belonging to three bidentate nitrate anions are in the range of 2.427(4)–2.690(4) Å. The bond angles of O1–Dy1–O2, O3–Dy1–O4, O2–Dy1–O4 and O1–Dy1–O3 are 63.96(11)°, 60.61(10)°, 96.40(12)° and 88.73(12)°, respectively. Notably, the crystal structure of **1** exhibits the broken hula hoop-like coordination geometry on Dy(III) sites (Figure 2, left). X-ray crystallographic analyses reveal that complex **2** crystallizes in the triclinic space group $P\bar{1}$ and possessing an asymmetric structure (Figure 1, right). Complex **2** consists of two Dy(III) ions, six nitrate anion, four H_2L ligands. Each Dy(III) ion is ligated by nine oxygen atoms from three H_2L^1 ligands and three bidentate nitrate anions, exhibiting a 9-coordinated tricapped trigonal prismatic geometry in the D_{3h} symmetrical coordination environment (Figure S4),[15] in which the bond distances of Dy1–O1, Dy1–O3 and Dy1–O12 of 2.345(4), 2.287(3) and 2.547(4) Å, respectively. However, the Dy2–O2, Dy2–O4 and Dy2–O7 distances are 2.315(13), 2.277(14), 2.341(15) Å. It suggests that the coordination field around

the Dy1(III) and Dy2(III) center is slightly different in complex **2.** Two Dy(III) ions are double bridged by four O atoms of four phenol oxygen atoms from two H_2L^1 ligands forming a $Dy_2L^1_2$ cycle with the Dy1···Dy2 distance of 9.3698 Å. Notably, the H_2L^1 ligand in complex **2** adopts two types of coordination modes, *e.g.* the bridging bidentate and monodentate (Scheme 1b), in which the nitrogen atoms remain uncoordinated. It is distinctively different from the hexa-dentate salen type Dy(III) complex **1** in which two crystallographically equivalent Dy(III) ions are bridged by only a pair of ligands in bidentate coordination modes forming a closed ring of $Dy_2L^2_2$ with the Dy···Dy distance of 10.098 Å. Strikingly, 9-coordinated Dy(III) ions in complex **2** demonstrates a hula hoop-like coordination geometry with the cyclic ring defined by the atoms O11, O17, O15, O3, O12 and O9 (Figure 2, right), while 10-coordinated Dy(III) ions in complex **1** display the broken hula hoop-like coordination geometry.

Complex **1** and **2** possess similar central $[Dy(H_2L)(NO_3)_3]_2$ and $[Dy(H_2L^1)_2(NO_3)_3]_2$ units, but consist different crystallization solvent molecules, complex **1** with one crystalline water molecule, one CH_3OH and CH_2Cl_2 solvent molecules, while complex **2** with two crystalline CH_3OH and CH_2Cl_2 solvent molecules. Such two salen type dinuclear structures with broken hula hoop-like and hula hoop-like coordination geometry are unique among the known salen type lanthanide complexes which are distinctively different from the reported salen type dinuclear complex $[Dy_2(L^3)_3(CH_3OH)]$ (H_2L^3 = *N,N'*-bis(salicylidene)-1,2-cyclohexaendiamine)[9] with a distorted sandwich structure. It also differs from the tetra-dentate salen type dinuclear complex $[Dy_2(L^4)_2(acac)_2(H_2O)]·2CH_2Cl_2$ (H_2L^4 = *N,N'*-bis(salicylidene)-1,2-cyclohexaendiamine, acac = acetylacetone)[7c] in which the two Dy(III) ions are bridged by two phenol oxygen atoms with a distance of 3.84 Å. In general, the "hula hoop" configuration may favor persistent axiality of Dy(III) ions, and the

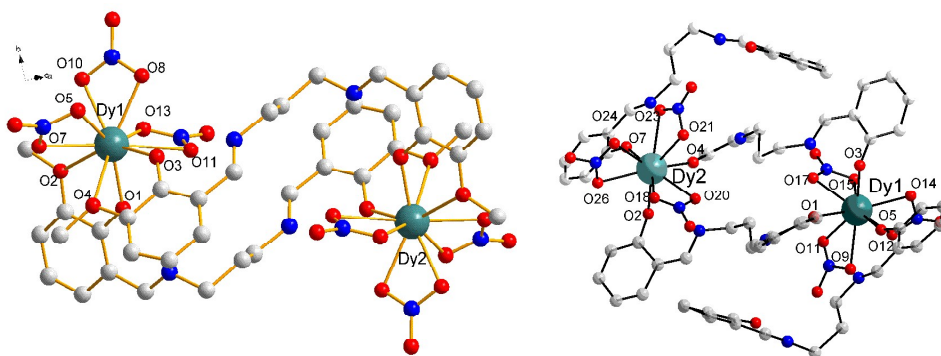orientations of easy axes achieve the efficient blockage of magnetization.[16]

Figure 1 Molecular structures of **1** (Left) and **2** (Right). (All hydrogen atoms are omitted for clarity)
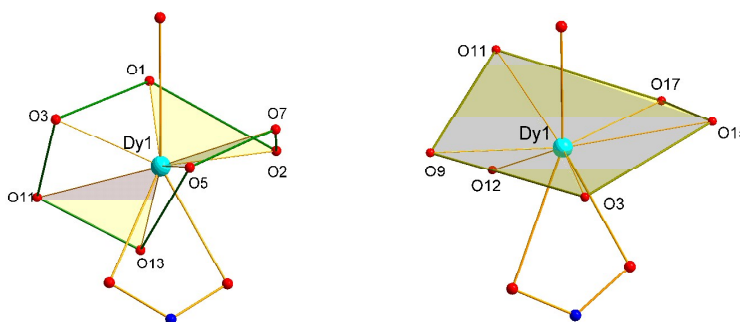

Figure 2 Broken hula hoop-like geometry for complex **1** (Left); Hula hoop-like geometry with the cyclic ring defined by the atoms O1, O11, O2, O13, O10, O8 for complex **2** (Right).

Magnetic properties

Magnetic measurements were performed on polycrystalline samples of complexes **1** and **2**. Direct current (dc) magnetic properties of complexes **1** and **2** were conducted under a 100 Oe field in the temperature range 300-1.8 K (Figure 3). The values of $\chi_m T$ at room temperature are 24.19 and 18.20 cm^3 K mol^{-1} for complexes **1** and **2**, respectively. These experimental values are smaller than the expected value of 28.34 cm^3 K mol^{-1} for two uncoupled Dy(III) ions, ($^6H_{15/2}$, $S = 5/2$, $L = 5$, $g = 4/3$, $\chi T = 14.17$ cm^3 K mol^{-1}), which high likely results from

the single-ion behavior of Dy(III) ions rather than from spin-spin coupling interactions between the Dy(III) ions.[17] For complexes **1** and **2**, followed by a slight decrease on lowering the temperature from 300 to 20 K and then drop sharply to reach a minimum of 18.33 and 14.23 cm^3 K mol^{-1} at 1.8 K. Therefore, the decrease is ascribed to the progressive depopulation of excited Stark sublevels, significant magnetic anisotropy or weak antiferromagnetic interactions present in the systems.[18]

The field dependence of the magnetization for complexes **1** and **2** was investigated in the range of 0 to 40 KOe at the temperatures 1.8, 3 and 5 K (Figure 3, inset). The magnetization increase rapidly at low field and then increase smoothly but without saturation even at 40 KOe. The magnetization eventually reaches the value of 8.03μ_B (for **1**), this value is lower than theoretical saturation value of 10.46μ_B (2×5.23μ_B), which high likely result from the crystal field effect around Dy(III) ions,[19] the magnetization eventually reaches the value of 10.20μ_B (for **2**) at 1.8 K which is in agreement with the expected value of 10.46μ_B (2×5.23μ_B).
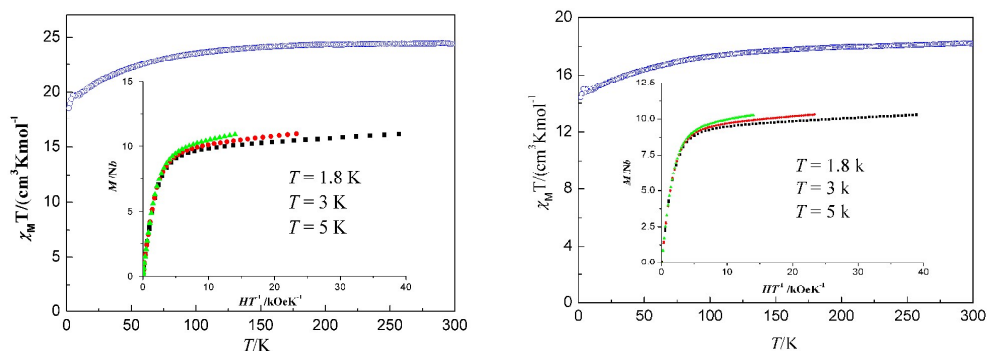

Figure 3 Temperature dependence of χ_MT for **1** (left) and **2** (right) at 100 Oe field. Inset: Plot of magnetization as a function of field for **1** and **2** at 1.8 K, 3K and 5K.

To further explore the magnetization dynamics, the alternating current (ac) susceptibility for complexes **1** and **2** were carried out in the frequency range of 1−1000 Hz. Complexes **1** and **2** displays clear frequency-dependent out-of-phase (χ'') signals at low temperatures under zero

dc magnetic field (Figure S5−S6), suggesting the existence of slow magnetic relaxation behavior.[20] The absence of any frequency-dependent peaks indicates the quantum tunneling of magnetization (QTM), which reduces the expected energy barrier in complexes **1** and **2**. In order to suppress the possible tunneling effects, an optimum field of 2000 Oe was applied. The slow magnetic relaxation peaks of out-phase signal (χ'') could be observed below 6 K in the frequency range of 10 Hz and 1000 Hz for **1** (Figure 4，left) and at the temperature range 3.5 K (100 Hz) to 5.5 (1000 Hz) for **2** (Figure 4, right) at 2000 Oe. In addition, an unconspicuous broad shoulder between 6 K (100 Hz) and 13 K (1000 Hz) is exhibited at 2000 Oe, which suggests the presence of two relaxation processes for **2**. To further confirm the relaxation processes in complex **2,** the frequency-dependent ac susceptibilities for **2** were run to further verify the relaxation dynamics under 2000 Oe dc field (Figure 5). There are two relaxation phases corresponding to the high-frequency signal (fast relaxation phase, FR) and the low-frequency region (slow relaxation phase, SR) in complex **2** (Figure 5, right).[21]
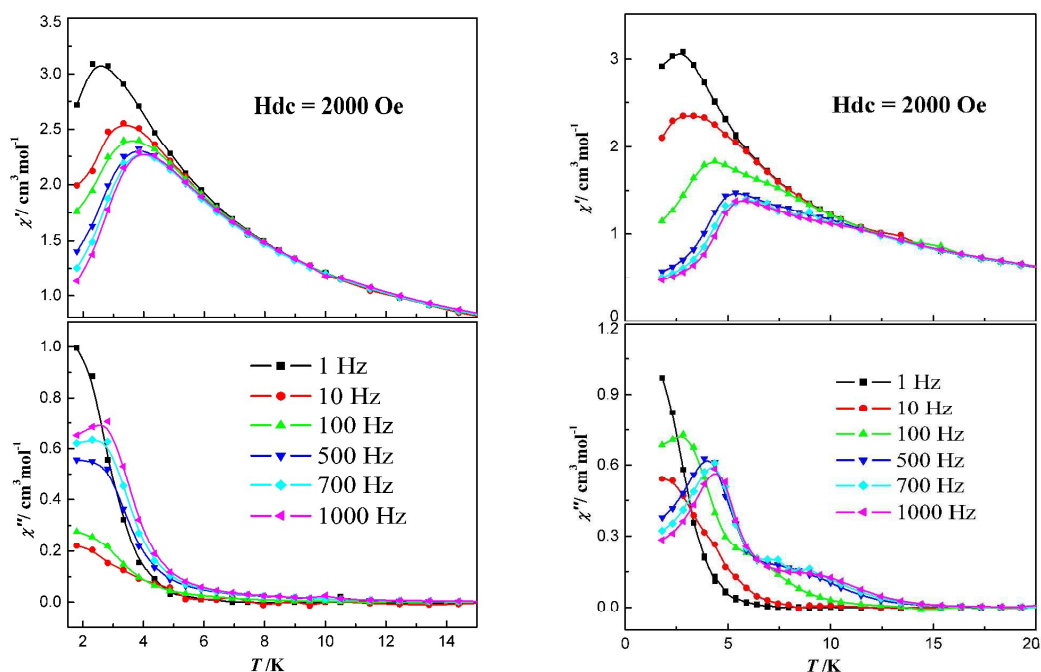

Figure 4 Temperature dependence of the in-phase (χ') and out-of-phase (χ'') ac susceptibility of **1** (left) and **2** (right) at 2000 Oe field in the frequency range 1–1000 Hz at 2–20 K.
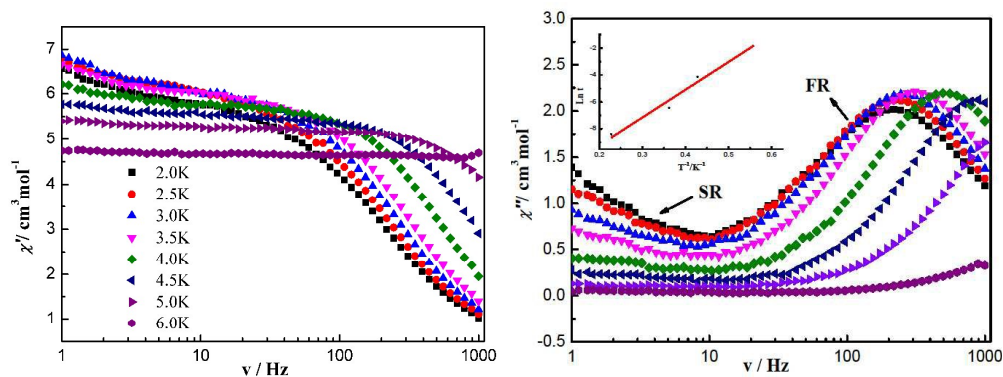
Figure 5 Frequency dependence of in-phase (χ') (left) and out-of-phase (χ'') (right) ac susceptibility of **2** at 2000 Oe field in the temperature range 2–6 K. The inset is the Arrhenius fit for the lnτ vs. T^{-1} plot.

The Cole-Cole plot under additional 2000 Oe dc field was conducted to further confirm the two relaxation processes in complex **2**. It shows semicircular shape and irregular curves in the high-frequency and low-frequency regions, which suggest existing more than one magnetic relaxation mode (Figure 6). The semicircular shape with raised tails is quite similar to that of a triple-decker salen type dinuclear complex [Dy(Pc)(acac)]$_2$·L^3 (Pc = phthalocyaninate, acac = acetylacetonate, H$_2$L^3 = (1s, 2s-*N*,*N*′-bis(5-bromo-2-hydroxylphenylmethene)-1,2-diphenylethylenediimine) at 2000 Oe field,[22] although differing from those of many distorted semi-circles shape. [7c, 7d]
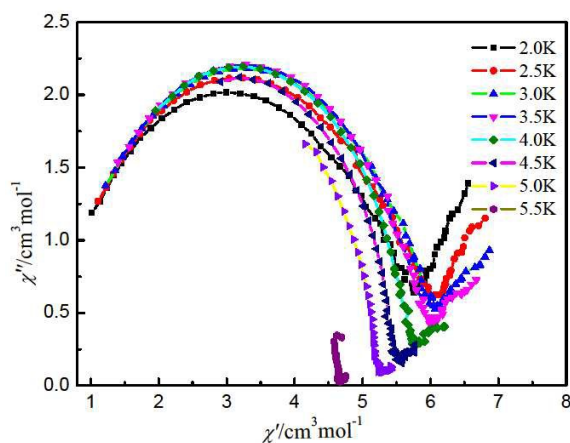
Figure 6 Cole–Cole plot for **2** obtained using the ac susceptibility data at 2000 Oe dc field in the temperature range 2–5.5 K.

On the basis of the Arrhenius relation [$\tau = \tau_0 \exp(U_{eff}/k_B T)$] [7d] and ac susceptibility data, the energy barriers (U_{eff}/k_B) can be caculated as 18.0 K and 43.0 K with a pre-exponential factors (τ_0) of 4.8×10^{-6} s and 3.0×10^{-6} s for **1** and **2**, respectively. (Figure S7 and Figure 5, inset)

Strikingly, the presence of two relaxation processes in complex **2** is unexpected as the two Dy(III) ions are of the same geometry. In general, the observation of two relaxation processes in dinuclear Dy(III) complexes were associated with the existence of anisotropic Dy(III) centres[21] and conformers.[22] However, two observed two relaxation processes may ascribed to the minute differences in bond lengths around two Dy(III) center which result in essential changes on the local anisotropy of the Dy(III) ions. Notably, the relatively higher energy barrier of complex **2** than complex **1** may result from the following two reasons. Firstly, the shorter bond length of Dy–O (2.446 Å) at the position of cyclic ring observed in hula hoop-like coordination geometry of complex **2** suggests the formation of a stronger ligand field on the local Dy(III) sites in complex **2** than bond length of Dy–O (2.454 Å) in complex **1**. The Dy(III) ions are located in the 9-coordinated geometry of tricapped trigonal prismatic geometry with D_{3h} symmetry in complex **2**, the high axiality of the Dy(III) ion achieved the efficient blockage of magnetization which enhance the SMMs behaviour.[19] In contrast, the Dy(III) ions in complex **1** is 10-coordinated with a distorted bi-capped square anti-prismatic geometry. The obvious disparity in magnetic dynamics should mainly result from the broken hula hoop-like coordination geometry in the Dy(III) ions, thus leading to the fast quantum tunneling from a more transverse anisotropy and relatively lower energy barrier. [7h]

In comparison with previously reported analogs, complex **2** reveals the relatively high effective energy barrier (U_{eff}) among the pure salen-type dinuclear dysprosium SMMs, e.g. $[Dy_2(HL^4)_4(CO_3)] \cdot 4H_2O$,[7h] $[Dy_2(L^5)_2(NO_3)_2(CH_3OH)_2] \cdot 4CH_3CN$,[7h] $[Dy_2(L^6)_2] \cdot 4CH_3CN$,[7g] and $[Dy_2L^7_3(CH_3OH)]$,[9] excerpt the serial salen-tye Dy$_2$ complexes by Long and co-workers,[7a, 7b,]

[7d] (Table 2). It can be concluded that the high axial coordination geometry around Dy(III) ions is enabling lanthanide complexes functioning as SMMs with high barrier such as the axial hula hoop-like geometry in complex **1** and the approximate D_{4d} in complexes $[Dy_2(valdien)_2](NO_3)_2]$, $(NEt_4)_2[Dy_2(L^2)_4](H_2O)(DMF)_{0.5}$ and $[Dy_2(valdien)_2](CF_3COCHCOCF_3)_2]$. Moreover, replacing H's with electron-withdrawing atoms on terminal salen-type ligands can be a relatively simple way of attaining higher barrier such as complexes $[Dy_2(L^5)_2(NO_3)_2(CH_3OH)_2]\cdot4CH_3CN]$, $[Dy_2(valdien)_2](NO_3)_2]$ and $[Dy_2(valdien)_2](CF_3COCHCOCF_3)_2]$.

Table 2 Differences of structural and magnetic parameters among complexes **1**, **2** and the reported pure Salen-type Dy$_2$ SMMs

Complexes	Coordination mode	Dy$_2$ core	Symmetry point group	U_{eff} value (K)	ref
1 [H$_2$L = N,N′-bis(2-hydroxy-3-methoxybenzylidene)-1,3-propanediamine]	O9	{DyO$_{10}$}	-----	18	-----
2 [H$_2$L^1 = N,N′-bis(salicylidene)-1,3-propanediamine]	O10	{DyO$_9$}	D_{3h}	43	-----
[Dy$_2$(HL^4)$_4$(CO$_3$)]·4H$_2$O [H$_2$L^4 = N′-((2-hydroxy-1-naphthyl)methylene)benzohydrazide]	N$_2$O$_6$	{DyO$_8$}	-----	17.4	8b
[Dy$_2$(L^5)$_2$(NO$_3$)$_2$(CH$_3$OH)$_2$]·4CH$_3$CN] [H$_2$L^5 = N′-((2-hydroxy-1-naphthyl)-methylene)picolinohydrazide]	N$_2$O$_6$	{DyO$_8$}	-----	41.2	8b
[Dy$_2$(L^6)$_2$]·4CH$_3$CN [[H$_2$L^6 = N$_1$, N$_2$, N$_3$, N$_4$-tri(3-methoxysalicydene)–triethylenetetraamine]	N$_3$O$_5$	{DyO$_8$}	-----	18.9	8a
Dy$_2$L^7$_3$(CH$_3$OH) [H$_2$L^7 = N,N′-bis(salicylidene)-1,3-cyclohecanediamine]	N$_4$O$_4$, N$_2$O$_5$,	{DyO$_8$}; {DyO$_7$}	-----	-----	10b
[Dy$_2$(valdien)$_2$](NO$_3$)$_2$ [H$_2$valdien = N$_1$,N$_3$-bis(-3-methoxysalicylidene)diet-hylenetriamine]	N$_3$O$_5$	{DyO$_8$}	D_{4h}	76	7f
(NEt$_4$)$_2$[Dy$_2$(L^2)$_4$](H$_2$O)(DMF)$_{0.5}$ [H$_2$L^2 = N,N′-bis(-3-methoxybenzylidene)-biphenyl-4,4′-diamine]	N$_3$O$_5$	{DyO$_8$}	D_{4h}	101	7d
[Dy$_2$(valdien)$_2$](CF$_3$COCHCOCF$_3$)$_2$] [H$_2$valdien = N$_1$,N$_3$-bis(-3-methoxysal-icylidene)diethylenetriamine]	N$_3$O$_5$	{DyO$_8$}	D_{4h}	110	7c

Conclusion

Isolation of complexes **1** and **2** demonstrates that synthesis of salen type dinuclear dysprosium complexes with *N,N'*-(1,3-propylene)bis(3-methoxysalicylideneimine) (hexadentate salen type) and *N,N'*-(1,3-propylene)bis(salicylideneimine)] (tetradentate salen type) are possible, and the structures of the salen type ligand dominate the structures of the complexes and the coordination geometries of the Dy(III) ions. The magnetic analysis suggests the hula hoop-like coordination geometry around each Dy(III) ions with a stronger ligand field lead to the typical SMM behavior with a higher energy barrier. The presence of two magnetic relaxations in complex **2** is associated with the presence of minute differences in bond lengths around Dy(III) center.

Acknowledgement

References

1   (a) X. Feng, Y. Li, Z. Zhang and E. Wang, *Acta. Chim. Sinica.*, 2013, **71**, 1575-1588; (b) Y.-N. Guo, G.-F. Xu, P. Gamez, L. Zhao, S.-Y. Lin, R. Deng, J. Tang and H.-J. Zhang, *J. Am. Chem. Soc.*, 2010, **132**, 8538-8539; (c) L. Sorace, C. Benelli and D. Gatteschi, *Chem. Soc. Rev.*, 2011, **40**, 3092-3104; (d) D. N. Woodruff, R. E. P. Winpenny and R. A. Layfield, *Chem. Rev.*, 2013, **113**, 5110-5148; (e) P.-F. Yan, P.-H. Lin, F. Habib, T. Aharen, M. Murugesu, Z.-P. Deng, G.-M. Li and W.-B. Sun, *Inorg. Chem.*, 2011, **50**, 7059-7065; (f) P.-P. Yang, X.-F. Gao, H.-B. Song, S. Zhang, X.-L. Mei, L.-C. Li and D.-Z. Liao, *Inorg. Chem.*, 2011, **50**, 720-722; (g) S.-Y. Zhou, X. Li, L. Tian, Z.-Y. Liu and X.-G. Wang, *RSC Adv.,* 2014, 5, 17131-17139; (h) L.-L. Li, S. Liu, H. Li, S. Wei and P. Cheng, *Chem. Commun.*, 2015, 51, 10933-10936; (i) Q.-P. Li and S.-W. Du, *RSC Adv.,* 2015,**5**, 9898-9903.

2   (a) C.-M. Liu, D.-Q. Zhang, and D. B. Zhu, *RSC Adv.,* 2015, 5, 63186-63192; (b) C.-B. Tian, D.-Q. Yuan, Y.-H. Han, Z.-H. Li, P. Lin and S.-W. Du, *Inorg. Chem. Front.*, 2014, **1**, 695-704;(c) A. Adhikary, H. S. Jena, S. Khatua and S. Konar, *Chem. Asian. J.*, 2014, **9**, 1083-1090; (d) Y.-N. Guo, G.-F. Xu, W. Wernsdorfer, L. Ungur, Y. Guo, J. Tang, H.-J. Zhang, L. F. Chibotaru and A. K. Powell, *J. Am. Chem. Soc.*, 2011, **133**, 11948-11951; (e) F. Habib, P.-H. Lin, J. Long, I. Korobkov, W. Wernsdorfer and M. Murugesu, *J. Am. Chem. Soc.*, 2011, **133**, 8830-8833; (f) A. K. Jami, V. Baskar and E. Carolina Sanudo, *Inorg. Chem.*, 2013, **52**, 2432-2438; (g) H.-H. Zou, R. Wang, Z.-L. Chen, D.-C. Liu and F.-P. Liang, *Dalton Trans.*, 2014, **43**, 2581-2587; (h) D.-K. Cao, R.-H. Wei, Y.-W. Gu, Y. Zhao and M. D. Ward. *RSC Adv.,*2014, **4**, 43064-43069.

3   R. J. Blagg, C. A. Muryn, E. J. L. McInnes, F. Tuna and R. E. P. Winpenny, *Angew. Chem. Int. Ed.*, 2011, **50**, 6530-6533.

4   (a) B. Hussain, D. Savard, T. J. Burchell, W. Wernsdorfer and M. Murugesu, *Chem. Commun.*, 2009, 1100-1102; (b) P. Zhang, L. Zhang, S.-Y. Lin, S. Xue and J. Tang, *Inorg. Chem.*, 2013, **52**, 4587-4592.

5   (a) X.-P. Yang, D. Schipper, R. A. Jones, L. A. Lytwark, B. J. Holliday and S.-M. Huang, *J. Am. Chem. Soc.,* 2013, 135, 8468-8471; (b) X.-P. Yang, R. A. Jones and S.-M. Huang, *Coord. Chem. Rev.,* 2014, 273-274,63-75; (c) X.-P. Yang, S.-Q. Wang, S.-M. Huang, D. Schipper and R. A. Jones, *Chem. Commun.,* 2014, 50, 15569-15572; (d) X.-P. Yang, M. Oye, R. A. Jones and S.-M. Huang, *Chem. Commun.,* 2013, 49, 9579-9581.

6   M. Yadav, V. Mereacre, S. Lebedkin, M. M. Kappes, A. K. Powell and P. W. Roesky, *Inorg. Chem.*, 2015, **54**, 773-781.

7.   (a) F. Habib, G. Brunet, V. Vieru, I. Korobkov, L. F. Chibotaru and M. Murugesu, *J. Am. Chem. Soc.*, 2013, **135**, 13242-13245; (b) F. Habib, J. Long, P.-H. Lin, I. Korobkov, L. Ungur, W. Wernsdorfer, L. F. Chibotaru and M. Murugesu, *Chem. Sci.*, 2012, **3**, 2158-2164; (c) P.-H. Lin, W.-B. Sun, M.-F. Yu, G.-M. Li, P.-F. Yan and M. Murugesu, *Chem. Commun.*, 2011, **47**, 10993-10995; (d) J. Long, F. Habib, P.-H. Lin, I. Korobkov, G. Enright, L. Ungur, W. Wernsdorfer, L. F. Chibotaru and M. Murugesu, *J. Am. Chem. Soc.*, 2011, **133**, 5319-5328;(e) H. Wang, C. Liu, T. Liu, S. Zeng, W. Cao, Q. Ma, C. Duan, J. Dou and J. Jiang, *Dalton Trans.*, 2013, **42**, 15355-15360; (f) L. Zhang, P. Zhang, L. Zhao, S.-Y. Lin, S. Xue, J. Tang and Z. Liu,

Eur. J. Inorg. Chem., 2013, 1351-1357; (g) L. Zhao, J. Wu, H. Ke and J. Tang, *Crystengcomm*, 2013, **15**, 5301-5306; (h) L. Zou, L. Zhao, P. Chen, Y.-N. Guo, Y. Guo, Y.-H. Li and J. Tang, *Dalton Trans.*, 2012, **41**, 2966-2971.

8   (a) M. Andruh, *Chem. Commun.*, 2011, **47**, 3025-3042; (b) X. Yang, C. Chan, D. Lam, D. Schipper, J. M. Stanley, X. Chen, R. A. Jones, B. J. Holliday, W.-K. Wong, S. Chen and Q. Chen, *Dalton Trans.*, 2012, **41**, 11449-11453.

9   J. Zhu, H. F. Song, P. F. Yan, G. F. Hou and G. M. Li, *Crystengcomm*, 2013, **15**, 1747-1752.

10   (a) A. Bhunia, M. A. Gotthardt, M. Yadav, M. T. Gamer, A. Eichhoefer, W. Kleist and P. W. Roesky, *Chem.-Eur. J.*, 2013, **19**, 1986-1995; (b) H. Ke, L. Zhao, Y. Guo and J. Tang, *Inorg. Chem.*, 2012, **51**, 2699-2705; (c) B. H. Koo, K. S. Lim, D. W. Ryu, W. R. Lee, E. K. Koh and C. S. Hong, *Chem. Commun.*, 2012, **48**, 2519-2521.

11   (a) T.-Q. Liu, P.-F. Yan, F. Luan, Y.-X. Li, J.-W. Sun, C. Chen, F. Yang, H. Chen, X.-Y. Zou and G.-M. Li, *Inorg. Chem.*, 2015, **54**, 221-228; (b) F. Luan, P. Yan, J. Zhu, T. Liu, X. Zou and G. Li, *Dalton Trans.*, 2015, **44**, 4046-4053; (c) J. Zhu, C. Wang, F. Luan, T. Liu, P. Yan and G. Li, *Inorg. Chem.*, 2014, **53**, 8895-8901.

12   J. P. Costes, F. Dahan and A. Dupuis, *Inorg. Chem.*, 2000, **39**, 165-168.

13   *CrysAlisPro, version 171.34.44*：Oxford Diffraction Ltd.: Oxfordshire, U.K., 2010.

14   (a) G. M. Sheldrick, *Sheldrick, SHELXL 97, Program for Crystal Structure Refinement, University of Göttingen: Göttingen, Germany* 1997; (b) G. M. Sheldrick, *Acta Crystallographica Section A*, 2008, **64**, 112-122.

15   H. Zhang, S.-Y. Lin, S. Xue, C. Wang and J. Tang, *Dalton Trans.*, 2014, **43**, 6262-6268.

16   Y.-N. Guo, X.-H. Chen, S. Xue and J. Tang, *Inorg. Chem.*, 2012, **51**, 4035-4042.

17   K. Katoh, Y. Horii, N. Yasuda, W. Wernsdorfer, K. Toriumi, B. K. Breedlove and M. Yamashita, *Dalton Trans.*, 2012, **41**, 13582-13600

18   N. L. Frank, R. Clerac, J. P. Sutter, N. Daro, O. Kahn, C. Coulon, M. T. Green, S. Golhen and L. Ouahab, *J. Am. Chem. Soc.*, 2000, **122**, 2053-2061.

19   Y.-N. Guo, X.-H. Chen, S. Xue and J. Tang, *Inorg. Chem.*, 2011, **50**, 9705-9713.

20   S. K. Langley, B. Moubaraki and K. S. Murray, *Inorg. Chem.*, 2012, **51**, 3947-3949.

21   M.-X. Yao, Q. Zheng, F. Gao, Y.-Z. Li, Y. Song and J.-L. Zuo, *Dalton Trans.*, 2012, **41**, 13682-13690.

22   S.-D. Jiang, S.-S. Liu, L.-N. Zhou, B.-W. Wang, Z.-M. Wang and S. Gao, *Inorg. Chem.*, 2012, **51**, 3079-3087.

Graphic Abstract
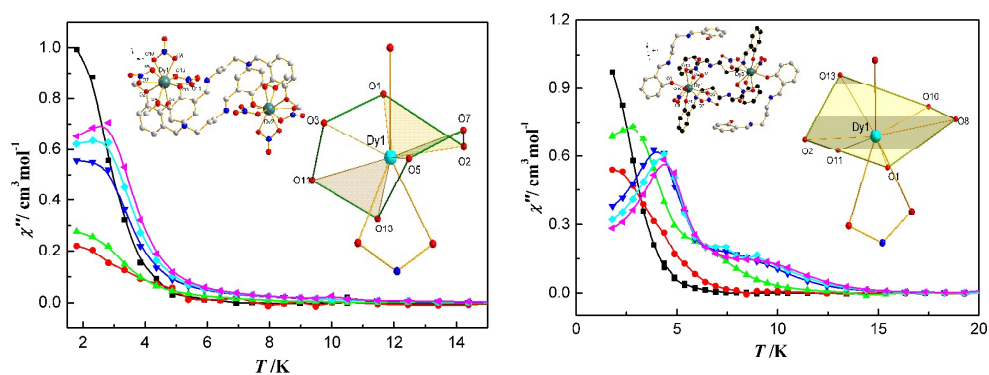
Two salen type dinuclear dysprosium complexes bridged by two ligands displaying the broken hula hoop-like and hula hoop-like coordination geometry have been isolated which show distinct magnetic properties of single and two magnetic relaxations.